

# Dalton Transactions

Accepted Manuscript



This is an *Accepted Manuscript*, which has been through the Royal Society of Chemistry peer review process and has been accepted for publication.

*Accepted Manuscripts* are published online shortly after acceptance, before technical editing, formatting and proof reading. Using this free service, authors can make their results available to the community, in citable form, before we publish the edited article. We will replace this *Accepted Manuscript* with the edited and formatted *Advance Article* as soon as it is available.

You can find more information about *Accepted Manuscripts* in the [Information for Authors](#).

Please note that technical editing may introduce minor changes to the text and/or graphics, which may alter content. The journal's standard [Terms & Conditions](#) and the [Ethical guidelines](#) still apply. In no event shall the Royal Society of Chemistry be held responsible for any errors or omissions in this *Accepted Manuscript* or any consequences arising from the use of any information it contains.

Cite this: DOI: 10.1039/c0xx00000x

www.rsc.org/xxxxxx

ARTICLE TYPE

## Bioinspired manganese(II) complexes with a clickable ligand for immobilisation on a solid support

Jérémy Chaignon,<sup>a,b</sup> Salah-Eddine Stiriba,<sup>a</sup> Francisco Lloret,<sup>a</sup> Consuelo Yuste,<sup>c</sup> Guillaume Pilet,<sup>d</sup> Laurent Bonneviot,<sup>b</sup> Belén Albela,<sup>\*b</sup> and Isabel Castro<sup>\*a</sup>

<sup>5</sup> Received (in XXX, XXX) Xth XXXXXXXXX 20XX, Accepted Xth XXXXXXXXX 20XX

DOI: 10.1039/b000000x

Clickable ligands like *N,N'*-bis((pyridin-2-yl)methyl)prop-2-yn-1-amine ( $L^1$ ) and *N*-((1-methyl-1H-imidazol-2-yl)methyl)-*N*-(pyridin-2-ylmethyl)prop-2-yn-1-amine ( $L^2$ ) have been used to synthesise a series of manganese(II) complexes for grafting on appropriate solid supports. These ligands mimic the 2-His-1-carboxylate facial chelation present in the active site of the manganese-dependent dioxxygenase (MndD), while the alkyne side function allows grafting the ligand in an azido-functionalised support using “click chemistry” methodologies. Such synthetic analogues of the MndD crystallise in the solid state as double halide or pseudohalide-bridged dinuclear manganese(II) complexes of general formula  $[Mn_2(\mu-X)_2X_2L_2]$  [ $L = L^1$  with  $X = Cl$  (**1**),  $Br$  (**2**), and  $N_3$  (**3**);  $L = L^2$  with  $X = N_3$  (**4**)]. Complexes **1–4** are characterised by a weak magnetic exchange interaction between the two high-spin  $Mn^{II}$  ions through the two  $X^-$  bridges ( $J$  in the range of  $-0.059$  to  $+5.30$   $cm^{-1}$ ,  $H = -J S_{Mn1} \cdot S_{Mn2}$  with  $S_{Mn1} = S_{Mn2} = 5/2$ ). A new magneto-structural correlation of superexchange bis( $\mu_{1,1}$ -azido)dimanganese(II) complexes has been proposed by using both structural parameters, the Mn–N–Mn bridging angle and the Mn– $N_{azido}$  distance. In MeOH-EtOH solution the dimeric species are present together with few percents of mononuclear manganese(II) complexes as evidenced by electron paramagnetic resonance (EPR) spectroscopy. Grafting the complexes in mesoporous silica of MCM-41 type stabilises both dimers and monomers in the nanopores of the solid.

### 20 Introduction

A natural evolution of bioinspired coordination chemistry is the immobilisation of metal complexes in solid supports where confinement can be created as in metalloproteins.<sup>1–3</sup> Fixation on a support allows not only achieving site isolation but also controlling site nuclearity. Indeed, for monomeric sites, oligomerisation and degradation are often observed in solution with molecular bioinspired complexes. Therefore, it is important to develop new ligands with side functions allowing reactions that are orthogonal to complexation for fixation on a solid support. One possibility is to use the Huisgen azide-alkyne [2+3] cycloaddition reaction referred to as “click chemistry” by Sharpless and co-workers.<sup>4</sup> Indeed, this efficient and versatile strategy, developed mainly for the synthesis of elaborated organic molecules (such as inhibitors for pharmaceutical applications), removes constraining considerations of protection/deprotection and cross-reactivity.<sup>5,6</sup> This synthetic strategy has been applied to graft molecules on various substrates such as organic polymers, carbon nanotubes, oxides and metals for the design of hybrid nanocomposite materials.<sup>7–9</sup> In the case of silica-based supports, either azide or alkyne functions are grafted on the solid support using the adequate organosiloxane molecule before carrying out the Huisgen cycloaddition reaction. In the case of immobilisation of a metal complex, it is preferred to have the alkyne function in the ligand and the azide in the tether to avoid complexation of azide to the metal ion. This modular approach has been used for example in the grafting of Co and V complexes with Schiff base ligands, or Pt and Pd organometallic complexes to develop

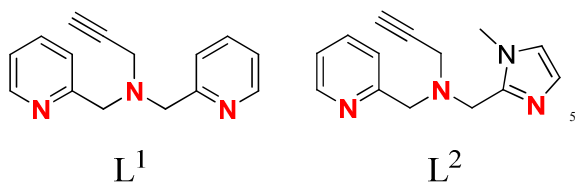
heterogeneous catalysts.<sup>10,11</sup>

Among metalloproteins, iron and manganese oxygenases are particularly attractive because they can perform oxidation of organic substrates by activating molecular oxygen.<sup>12–19</sup> In particular, catechol dioxxygenases are ring-cleaving enzymes that oxidise catechol derivatives with a concomitant ring opening, which is a critical step in the aerobic degradation of aromatic compounds by bacteria.<sup>19</sup> Therefore, these systems can be used as models to develop new materials for the degradation of aromatic chemicals. For instance, manganese-dependent dioxxygenase (MndD) is known to catalyse the extradiol cleavage of catechol derivatives.<sup>15–18,20</sup> The active site of this metalloprotein contains a mononuclear manganese centre coordinated to two histidines (His) and one glutamate (Glu) or one aspartate (Asp) in facial position.<sup>21–23</sup> This motif, called the 2-His-1-carboxylate facial triad, is observed in catechol dioxxygenases as well as in other metalloproteins.<sup>15,24</sup>

In this work a new series of manganese complexes with the two different biomimetic clickable ligands *N,N'*-bis((pyridin-2-yl)methyl)prop-2-yn-1-amine ( $L^1$ ) and *N*-((1-methyl-1H-imidazol-2-yl)methyl)-*N*-(pyridin-2-ylmethyl)prop-2-yn-1-amine ( $L^2$ ) is presented (Scheme 1). Both ligands can mimic the facial triad present in the active site of the MndD and possess an alkyne side function that allows for an efficient grafting in a solid support using click chemistry.

We report herein the crystal structures and the magnetic properties of four novel manganese(II) complexes of formula  $[Mn_2(L^1)_2Cl_2(\mu-Cl)_2]$  (**1**),  $[Mn_2(L^1)_2Br_2(\mu-Br)_2]$  (**2**),  $[Mn_2(L^1)_2(N_3)_2(\mu_{1,1}-N_3)_2] \cdot 2CH_3OH$  (**3**), and  $[Mn_2(L^2)_2(N_3)_2(\mu_{1,1}-$

$N_3)_2]$  (**4**). The grafting is exemplified by the reaction of **1** with a mesoporous silica (MCM-41 type) modified with azide functions.

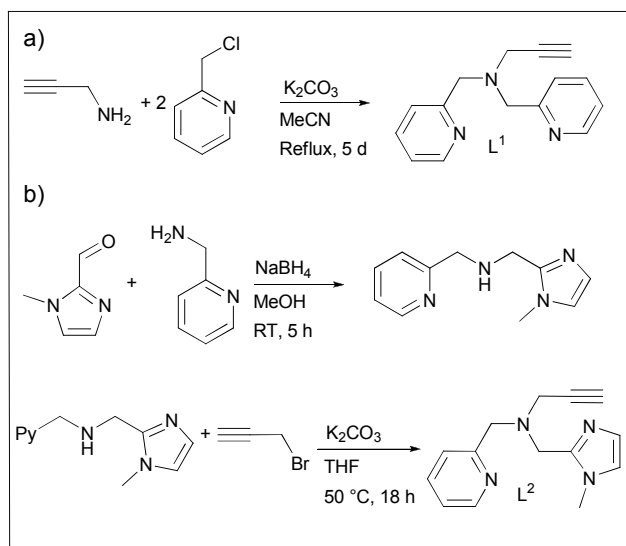


**Scheme 1.** Representation of ligands  $L^1$  and  $L^2$ . Nitrogen atoms involved in the coordination of the metal ion are highlight in red.

## 10 Results and discussion

### Synthesis of the ligands

The ligands  $L^1$  and  $L^2$  were synthesised according to experimental procedures reported in the literature. In the case of  $L^1$ , two different synthetic methods were explored. The first one is a two-step protocol starting with the reduction by  $NaBH_4$  of the Schiff base resulting from the condensation of the 2-picolylamine with the 2-pyridinecarboxaldehyde which is followed by an electrophilic substitution with propargyl bromide to obtain the desired  $L^1$  ligand.<sup>25, 26</sup> The yield of the first step was 96% with a simple work-up whereas the purification by column chromatography on silica for the second step only yielded 11% of the product likely due to the less affinity of amino-pyridinic substrates to the acidic nature of the silica. Yet this latter should not be taken as a standard reaction yield as results found in the literature report average yields around 90%.<sup>27</sup>



**Scheme 2.** a) Synthesis of ligand  $L^1$  and b) synthesis of ligand  $L^2$ .

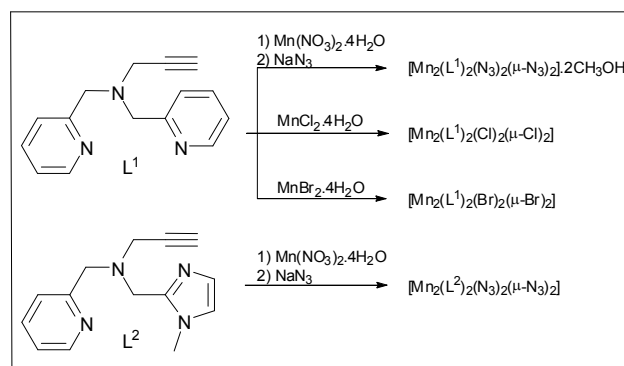
The second method is a straightforward one-step protocol consisting in a double electrophilic substitution involving propargylamine and 2-picolyl chloride.<sup>28</sup> Reaction time of 12 h was prolonged up to 5 days allowing us to retrieve  $L^1$  in a 90 to 96 % yield, compared to a 32 % yield for 12 h. Therefore this one-step protocol was the appropriate synthetic route for  $L^1$  ligand (Scheme 2a).

$L^2$  is an original ligand that has been synthesized using an

adapted version of the previous first method, *i.e.*, condensation of an amine and an aldehyde, namely 2-picolylamine and 1-methyl-2-imidazolecarboxaldehyde, respectively, followed by a reduction<sup>29</sup> and an electrophilic substitution by propargyl bromide (Scheme 2b). The first step provided the secondary amine in a 96 % yield. It is interesting to note the absence of undesired by-products in the second step, contrary to the synthesis of  $L^1$  that required purification by column chromatography. In fact, redissolution in  $CH_2Cl_2$  and filtration through KBr provided the pure ligand  $L^2$  in 80 % yield.

### Synthesis of the Mn(II) complexes

Complexes **1–4** were synthesized in MeOH by using a stoichiometric amount of ligand and metal salt (Scheme 3). For compounds **1** and **2** involving chloride and bromide counter-anions respectively, the corresponding manganese salt was available and directly used for the reaction. In the case of **3** and **4**, involving azide anions, manganese nitrate was reacted with the ligand and 4 equivalents of sodium azide were added to exchange the nitrate anion by the azide one. Except for **2**, each compound precipitated as light brown powder in MeOH within 30 min. Those powders were then redissolved in the minimum amount of MeOH, while the solution containing **2** was used as it is. The growth of crystals was performed using the same technique in all the cases, *i.e.*, slow diffusion of diethyl ether in a methanolic solution of the compound, to afford crystals within a couple of days. Apart from **3**, all the crystals were stable in air at room temperature. Molecules of MeOH found in the structure of **3** were loosened when left at room temperature, damaging the crystallinity of the solid.



**Scheme 3.** Synthesis of the manganese(II) complexes.

### 70 Description of the structures

Complexes **1–4** are double halide or pseudohalide-bridged neutral dimers of Mn(II) and exhibit the same structural layout (Fig. 1). They differ by the nature of the donor groups from the organic ligand counterpart, *i.e.*, amine and pyridines from  $L^1$  (**1–3**), or amine, pyridine and imidazole from  $L^2$  (**4**), as well as the coordinating anion composing the double bridge between the metal ions and completing the metal environments, *i.e.*, chloride (**1**), bromide (**2**), or azide (**3** and **4**). Selected bond distances and angles for **1–4** are compiled in Table 1.

**Table 1.** Selected bond distances (Å) and angles (°)

	1	2	3	4
Mn(1)–N(1)	2.280(4)	2.264(2)	2.255(2)	2.296(1)
Mn(1)–N(2)	2.272(3)	2.269(2)	2.265(2)	2.192(2)
Mn(1)–N(3)	2.388(3)	2.389(2)	2.384(2)	2.466(2)
Mn(1)–X(1) <sup>a</sup>	2.515(2)	2.6641(5)	2.225(2)	2.231(1)
Mn(1)–X(2) <sup>a</sup>	2.423(1)	2.5740(5)	2.153(2)	2.131(2)
Mn(1)–X(1) <sup>a</sup>	2.574(1)	2.7333(5)	2.244(2)	2.209(1)
Mn⋯Mn	3.827(1)	4.0076(5)	3.533(3)	3.486(3)
Mn–X(1)–Mn <sup>a</sup>	97.52(4)	95.88(1)	104.50(6)	103.47(6)

<sup>a</sup>1: X = Cl; 2: X = Br; 3 and 4: X = N<sub>3</sub>.

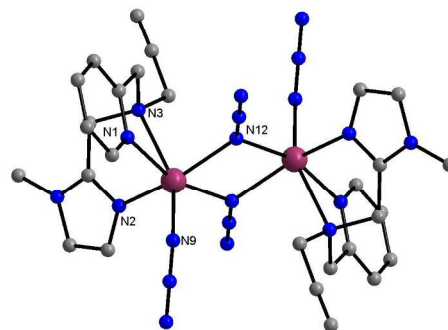
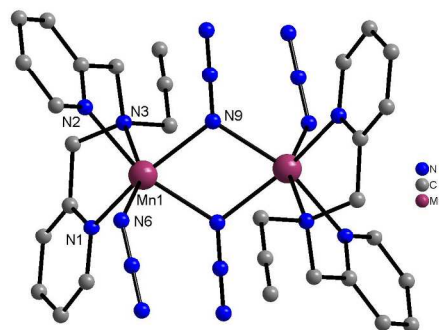
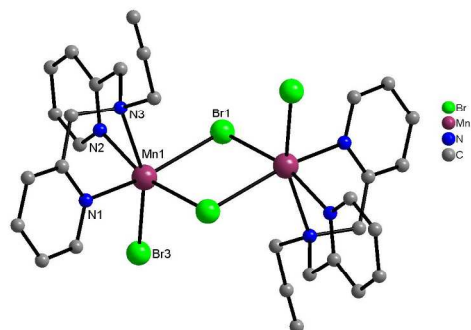
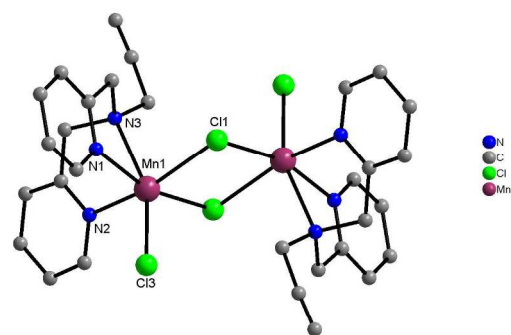
Within all complexes, the Mn(II) ions are located in a distorted N<sub>3</sub>X<sub>3</sub> [X = Cl (1), Br (2) and N (3 and 4)] octahedral environment. In all the complexes, the Mn–N bond lengths from the tridentate ligands are similar and in good agreement with similar complexes involving double bridge with double chloride,<sup>30–32</sup> bromide<sup>33</sup> and end-on azide<sup>34–37</sup> bridges. It is important to note that the Mn–N bond length involving the central amine nitrogen atom of the ligand is usually ~0.1 Å longer than the two external ones involving the pyridine and/or imidazole nitrogen atoms. In the case of 4, involving L<sup>2</sup>, one of the Mn–N bond lengths (N2) or the external nitrogen atoms of the ligand is shorter (~0.1) and the Mn–N bond length for the central (N3) one is longer (~0.1 Å) than those observed for complexes 1–3 involving L<sup>1</sup>. The environment of the metal ions is completed by three X atoms with two of which involved in the double bridge between the two Mn(II) ions. As expected, Mn–Cl bond lengths are shorter than the Mn–Br ones. Moreover, Mn–X bond lengths within the double bridge (X = Cl1, Br1) are longer (~0.1 Å) than the terminal ones (X = Cl3, Br3).

The distortion of the octahedral environment of the metal ion is also exemplified by the distribution, far from the ideal values of 90 and 180°, of the X–Mn–X angles (X = N, Br and Cl) ranging from 69.72(5)° to 104.193(16)° and from 158.24(3)° to 163.59(4)° for 1; from 71.45(8)° to 101.689(15)° and from 159.85(5)° to 165.10(6)° for 2; from 72.86(5)° to 105.08(6)° and from 154.43(6)° to 163.57(6)° for 3; from 69.79(4)° to 103.22(7)° and from 154.83(6)° to 161.98(5)° for 4.

In the crystal lattice of 1 and 2, structural packing is built by weak hydrogen bonding H⋯X (X = Cl and Br, respectively) interactions leading to a dense 3D network. In case of 3, the co-crystallized methanol molecule, through the hydrogen atom of the alcoholic group, forms hydrogen bonds with the terminal nitrogen atom of the double end-on azido-bridge. Finally, for 3 and 4, the crystal packing, in both cases, is assumed by weak interactions as Van der Waals ones for example.

#### 40 Magnetic properties

Fig. 2 shows the magnetic properties of 1–4 in the form of the  $\chi_M T$  versus  $T$  plots and  $M$  versus  $H$  plots,  $\chi_M$  and  $M$  being the magnetic susceptibility and the magnetisation per two Mn(II) ions respectively, while  $T$  and  $H$  are the absolute temperature and the applied magnetic field, respectively.

**Fig. 1** Structures of Mn(II) complexes with L<sup>1</sup> and L<sup>2</sup> ligands 1–4.

At room temperature,  $\chi_M T$  for 1 and 2 is ca. 8.75 cm<sup>3</sup> mol<sup>-1</sup> K. Whereas this value is expected for two magnetically isolated high-spin Mn<sup>II</sup> ions ( $S_{Mn} = 5/2$ ), the corresponding values for 3 and 4 are somewhat greater (ca. 9.5 cm<sup>3</sup> mol<sup>-1</sup> K). Upon cooling,  $\chi_M T$  for 1 remains constant until 25.0 K and it further decreases to 7.70 cm<sup>3</sup> mol<sup>-1</sup> K at 2.0 K, suggesting the occurrence of a very weak antiferromagnetic interaction. In contrast,  $\chi_M T$  for 2–4 continuously increases with the decrease of the temperature to reach maxima at 5.5 K (ca. 11.3 cm<sup>3</sup> mol<sup>-1</sup> K) for 2 and at 10 K



(ca. 14.8 cm<sup>3</sup> mol<sup>-1</sup> K) for **3** and **4**. After these maxima,  $\chi_M T$  decreases to 7.5 (**2**), 13.7 (**3**) and 13.9 cm<sup>3</sup> mol<sup>-1</sup> K (**4**) at 2.0 K. The increase of  $\chi_M T$  in the high temperature region for **2–4** is indicative of the occurrence of a ferromagnetic interaction

between the paramagnetic Mn(II) ions, whereas the decrease at low temperatures can be attributed to weak intermolecular antiferromagnetic interactions and/or zero-field splitting of the  $S = 5$  ground spin state. However, because of the large isotropic character of the six-coordinate high-spin Mn(II) ion, the zero-field splitting effects are expected to be negligible.

The expression of the magnetic susceptibility for a dimanganese(II) unit derived from the Van Vleck's equation (the spin Hamiltonian being defined as  $H = -J\mathbf{S}_{Mn1} \cdot \mathbf{S}_{Mn2}$ ) is given by eq (1),<sup>38</sup>

$$\chi_M = \frac{2Ng^2\beta^2}{k(T-\theta)} \frac{e^x + 5e^{3x} + 14e^{6x} + 30e^{10x} + 55e^{15x}}{1 + 3e^x + 5e^{3x} + 7e^{6x} + 9e^{10x} + 11e^{15x}} \quad (1)$$

where  $x = J/kT$  and  $\theta$  is the Weiss constant defined as  $\theta = zJ'S(S+1)/3k$  with  $zJ'$  accounting for the magnetic interaction between the  $z$  nearest dinuclear units. The other parameters have their usual meaning. The best-fit parameters obtained are listed in

Table 2.

**Table 2.** Best-fit parameters for **1–4** (see text)

Compound	$g$	$J / \text{cm}^{-1}$	$zJ' / \text{cm}^{-1}$
<b>1</b>	1.99(1)	-0.059(1)	0.0
<b>2</b>	1.99(1)	+1.04(2)	-0.20(1)
<b>3</b>	2.01(1)	+5.30(4)	-0.060(2)
<b>4</b>	2.02(1)	+4.99(3)	-0.052(2)

As indicated above, the decrease of  $\chi_M T$  at low temperatures for **2–4** could be alternatively interpreted by the presence of a zero-field splitting ( $D$ ). Having this possibility in mind, the magnetic data for **2–4** were also analysed through the Hamiltonian of eq (2) by using VPMAG.<sup>39</sup>

$$H = -J\mathbf{S}_{Mn1} \cdot \mathbf{S}_{Mn2} + D(S_{zMn1}^2 + S_{zMn2}^2 + 35/6) \quad (2)$$

The least-squares fit of the experimental data to eq (2) gave values for the  $g$  and  $J$  parameters similar to those obtained through eq (1) (Table 2), but the values for the  $D$  parameter [4.9 (**2**), 1.4 (**3**) and 1.1 cm<sup>-1</sup> (**4**)] are too high to be considered real and they are meaningless. In fact, the reported  $D$  values for the high-spin d<sup>5</sup> Mn<sup>II</sup> ion in an octahedral environment are lower than

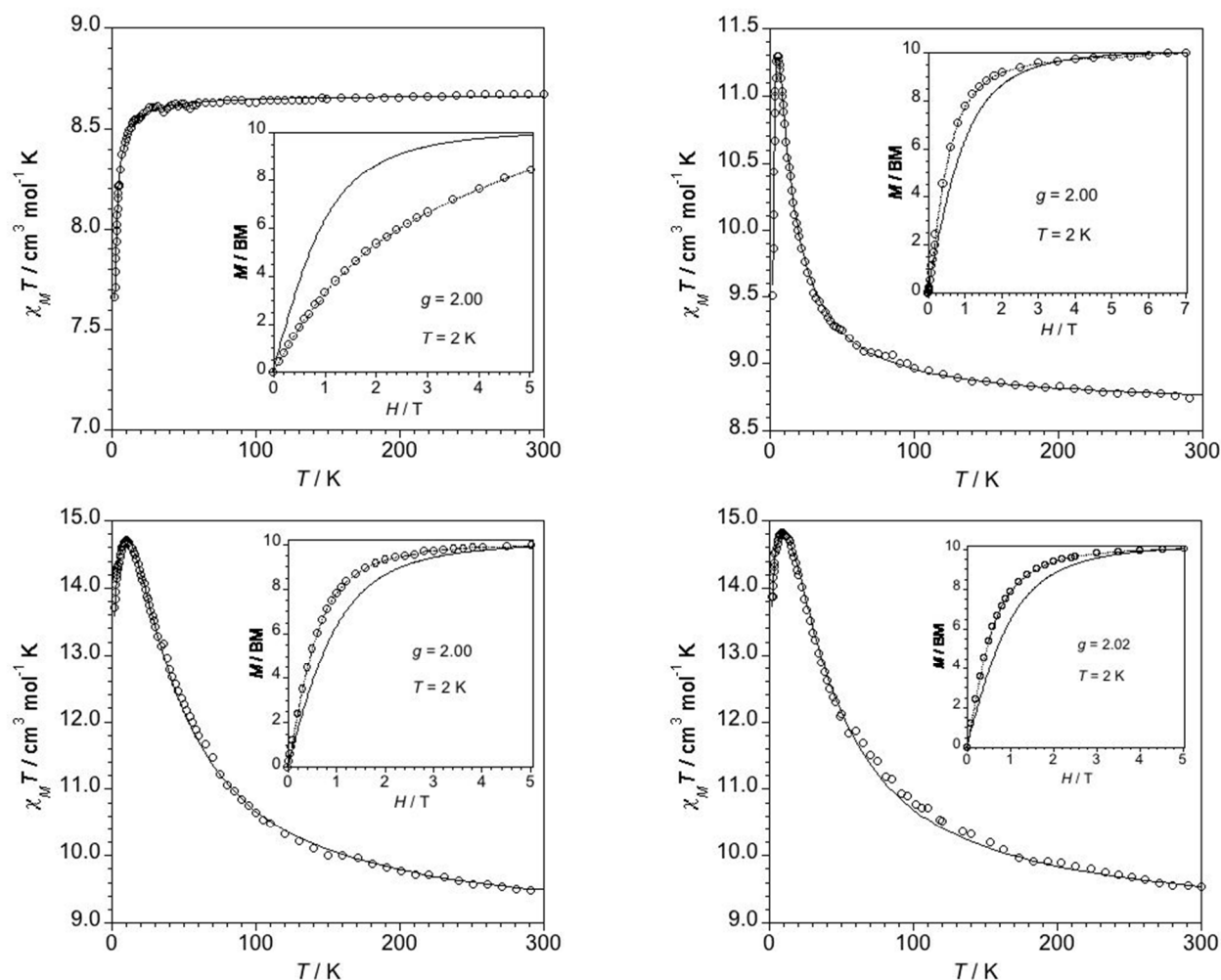


**Fig. 2** Temperature dependence of  $\chi_M T$  for **1** (top left), **2** (top right), **3** (bottom left) and **4** (bottom right). The solid line represents the best fit based on the parameters discussed in the text (Table 2). The inset shows the magnetization curve at 2.0 K and the solid line is the theoretical Brillouin curve for two magnetically independent spin sextuplets,  $S = 5/2$ .

1  $\text{cm}^{-1}$ .<sup>40</sup> So, the decrease of the  $\chi_M T$  values has to be mainly attributed to intermolecular antiferromagnetic interactions.

Field dependence magnetisation plots of **1–4** at 2.0 K are shown in the inset of the corresponding plot (Fig. 2). The isothermal magnetisation data for **1** are well below the Brillouin curve for two magnetically isolated  $S = 5/2$  Mn(II) ions (with no ZFS), while they are well above for **2–4**, in agreement with the occurrence of antiferro- (**1**) or ferromagnetic (**2–4**) interactions between the Mn(II) ions.

The main magneto-structural parameters for a series of  $[\text{Mn}^{\text{II}}(\mu\text{-X})_2\text{Mn}^{\text{II}}]$  ( $X = \text{Cl}$  or  $\text{Br}$ ) dinuclear complexes which were subject of previous studies are gathered in Table 3. As far as we know, no theoretical magneto-structural correlation has been reported for this family. As one can see therein, no correlation seems to exist between the structural parameters (angles or distances) and magnetic coupling parameter ( $J$ ), this circumstance being most likely due to the scarce number of compounds, the small variation of the structural parameters and the experimental errors. However, there must exist a correlation between the nature and magnitude of the magnetic exchange and the structural parameters, the value of the Mn–X–Mn angle being the most determinant one, as it is known for other metal ions and bridging ligands.<sup>41</sup> In fact, the experimental data from Table 3, predict a change from ferro- to antiferromagnetic behaviour at an angle of *ca.*  $97^\circ$  for the bridgehead chloro atom. The value of this crossover Mn–Cl–Mn angle is very close to that observed for the bis( $\mu$ -hydroxo)dicopper(II) complexes (*ca.*  $97.5^\circ$ ).<sup>41</sup> Compound **2** is the first example of a bis( $\mu$ -bromo)dimanganese(II) complex studied for its magnetic properties and so, we can only compare it with the chloro derivatives listed in Table 3.

**Table 3.** Selected magneto-structural parameters for bis( $\mu$ -X)dimanganese(II) complexes ( $X = \text{Cl}$  or  $\text{Br}$ )

Compound <sup>a</sup>	$d_{\text{Mn-Mn}}/\text{\AA}$	$d_{\text{Mn-Cl}}/\text{\AA}$	Mn–X–Mn/ <sup>o</sup>	$J/\text{cm}^{-1}$	Ref.
$[\text{Mn}_2(\text{biz})_2(\mu\text{-Cl})_2]\text{Cl}_2$	3.74	2.57	93.5	+0.66	<sup>32</sup>
$[\text{Mn}_2(\text{bpea})_2\text{Cl}_2(\mu\text{-Cl})_2]$	3.79	2.48	95.7	+0.68	<sup>30</sup>
$[\text{Mn}_2(\text{mpba})_2\text{Cl}_2(\mu\text{-Cl})_2]$	3.9	2.50	96.4	+1.1	<sup>31</sup>
<b>1</b>	3.82	2.54	97.5	–0.06	t. w.
<b>2</b>	4.00	2.69	95.9	+1.04	t. w.

<sup>a</sup>Abbreviations: biz = 2,2'-biimidazole; bpa = *N,N'*-bis(2-pyridylmethyl) ethylamine; mpbpa = *N*-(3-methoxypropyl)-*N,N'*-bis(pyridin-2-ylmethyl) amine; L<sup>1</sup> = see text; t. w. = this work.

Concerning the bis( $\mu_{1,1}$ -azido)dimanganese(II) complexes (**3** and **4**), an experimental relationship between the magnetic coupling ( $J$ ) and the Mn–N–Mn bridging angle ( $\theta$ ),  $J(\text{cm}^{-1}) = 0.552\theta(\text{deg}) - 53.8$ , was proposed.<sup>36, 43</sup> Table 4 shows the magneto-structural parameters for double end-on azido-bridged Mn(II) complexes. **3** and **4** follow roughly the above relationship and they are in good agreement with the fact that the value of the exchange coupling constant increases with the Mn–N–Mn bridging angle, which is consistent with theoretical predictions.<sup>41</sup> A careful inspection of the data listed in Table 4 shows that the values of the coupling parameter,  $J$ , generally increase with an increase in the difference between the two Mn–N(bridging azide) bond distances ( $\Delta d$  in Table 4),<sup>36, 43</sup> that is an increase in the asymmetry of the azido bridging. In this sense, a better magneto-structural correlation is observed when we use both structural parameters ( $\theta$  and  $\Delta d$ ). Fig.

3 shows the values of  $J$  versus the corresponding values of  $(\theta + 10\Delta d)$  from Table 4. The best linear fit gives the equation  $J(\text{cm}^{-1}) = 0.553[\theta(\text{deg}) + 10\Delta d(\text{\AA})] - 54.111$ , which is slightly better than  $J(\text{cm}^{-1}) = 0.576\theta(\text{deg}) - 54.040$ , where the influence of  $\Delta d$  has been neglected.

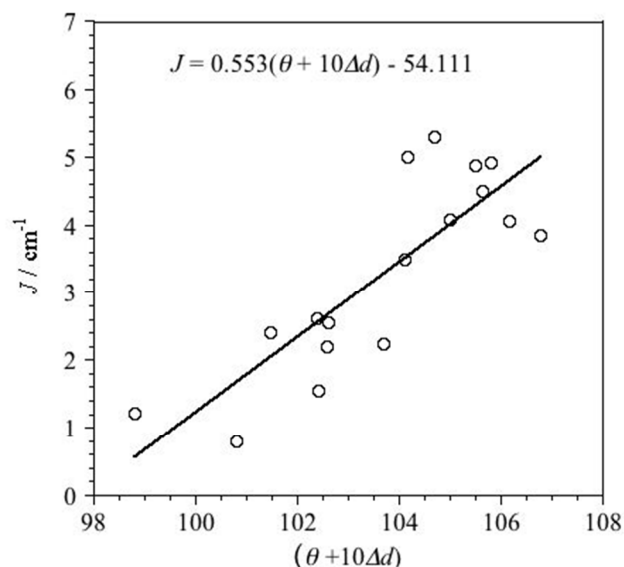


**Fig. 3** Plot of  $J$  versus  $(\theta + 10\Delta d)$ ,  $\theta$  being the average Mn–N–Mn angles and  $\Delta d$  the average Mn–N(azido-bridge) bond distances (see text), for double end-on azido-bridged Mn(II) complexes (see Table 3). The solid straight line represents the best linear fit to equation  $J = 0.553(\theta + 10\Delta d) - 54.111$ .

**Table 4.** Selected magneto-structural parameters for bis( $\mu_{1,1}$ -azido)dimanganese(II) complexes<sup>(a)</sup>

Compound	$\Delta d/\text{\AA}$	$\theta/\text{deg}$	$\theta+10\Delta d$	$J/\text{cm}^{-1}$	Ref.
$[\text{Mn}_2(\text{ttp})_2(\text{N}_3)_2(\mu_{1,1}\text{-N}_3)_2]$	0.236	103.45	105.81	4.92	36
$[\text{Mn}_2(\text{ttp-N}_3)_2(\text{N}_3)_2(\mu_{1,1}\text{-N}_3)_2]$	0.252	103.13	105.65	4.50	36
$[\text{Mn}_2(\text{ttp-N}_3)_2(\text{N}_3)_2(\mu_{1,1}\text{-N}_3)_2]_2[\text{Mn}(\text{ttp-N}_3)(\text{N}_3)_3]$	0.150	105.29	106.79	3.84	36
$[\text{Mn}_2(\text{terpy})_2(\text{N}_3)_2(\mu_{1,1}\text{-N}_3)_2]\cdot 2\text{H}_2\text{O}$	0.090	104.60	105.50	4.86	44
$[\text{Mn}_2(\text{L}^{\text{A}})_2(\mu_{1,1}\text{-N}_3)_2](\text{ClO}_4)_2$	0.030	102.12	102.42	1.54	43
$[\text{Mn}_2(\text{L}^{\text{B}})_2(\mu_{1,1}\text{-N}_3)_2](\text{ClO}_4)_2$	0.072	104.29	105.01	4.09	43
$[\text{Mn}_2(\text{L}^{\text{C}})_2(\mu_{1,1}\text{-N}_3)_2](\text{ClO}_4)_2$	0.053	103.58	104.11	3.50	43
$[\text{Mn}_2(\text{phen})_4(\mu_{1,1}\text{-N}_3)_2][\text{Co}(\text{bpb})(\text{CN})_2]\cdot 2\text{H}_2\text{O}$	0.002	102.60	102.62	2.54	45
$[\text{Mn}_2(\text{phen})_4(\mu_{1,1}\text{-N}_3)_2][\text{Cr}(\text{bpb})(\text{CN})_2]\cdot 2\text{H}_2\text{O}$	0.003	102.55	102.58	2.20	45
$[\text{Mn}_2(\text{phen})_4(\mu_{1,1}\text{-N}_3)_2][\text{Fe}(\text{bpb})(\text{CN})_2]\cdot 2\text{H}_2\text{O}$	0.006	101.40	101.46	2.40	45
$[\text{Mn}_2(2,2'\text{-dpa})_2(\text{N}_3)_2(\mu_{1,1}\text{-N}_3)_2]$	0.059	103.11	103.70	2.24	34
$[\text{Mn}(\text{tptz})(\mu_{1,1}\text{-N}_3)_2]_n$	0.002	106.16	106.18	4.06	46
$[\text{Mn}(\text{pyz})(\mu_{1,1}\text{-N}_3)_2]$	0.000	98.80	98.800	1.22	47
$[\text{Mn}(2\text{-bzpy})(\mu_{1,1}\text{-N}_3)_2]_n$	0.032	100.50	100.82	0.80	48
$[\text{Mn}_2\text{L}^{\text{D}}(\text{N}_3)_2(\mu_{1,1}\text{-N}_3)_2]$	0.202	100.38	102.40	2.62	37
<b>3</b>	0.019	104.50	104.69	5.30	t. w.
<b>4</b>	0.020	103.96	104.16	4.99	t. w.

(a) Average values.  $\Delta d = d(\text{Mn}-\text{N}_{\text{azido}}) - d(\text{Mn}-\text{N}'_{\text{azido}})$ . ttp = 4'-p-Tolyl-2,2':6',2''-terpyridine, ttp-N<sub>3</sub> = 4'-p-Azidomethylphenyl-2,2':6',2''-terpyridine, L<sup>A</sup> = [N,N-bis(pyridine-2-yl)benzylidene]ethane-1,2-diamine, L<sup>B</sup> = [N,N-bis(pyridine-2-yl)benzylidene]propane-1,3-diamine, L<sup>C</sup> = [N,N-bis(pyridine-2-yl)benzylidene]butane-1,4-diamine, bpb<sup>2-</sup> = 1,2-bis(pyridine-2-carboxamido)benzenate, 2,2'-dpa = 2,2'-dipicolylamine, tptz = 2,4,6-tris(2-pyridyl)-1,3,5-triazine, pyz = pyrazine, 2-bzpy = 2-benzoylpyridine, L<sup>D</sup> = 2-(benzimidazol-2-yl)-N-(pyridin-2-ylmethyl)ethanamine

### EPR characterization of the complex in solution

The molecular complex **1** is conveniently dissolved in MeOH/EtOH solution. Such a solution exhibits at room temperature a 6 lines EPR signal centered at  $g = 2.001 \pm 0.001$  typical of Mn(II). It is assigned to the hyperfine coupling between the electronic spin ( $S = 5/2$ ) and the nuclear manganese spin ( $I = 5/2$ ) for the allowed transitions ( $\Delta m_S = \pm 1$ ,  $\Delta m_I = 0$ ). Upon simulation, the hyperfine coupling constant  $A$  is  $97 \pm 1$  G (Fig. S5). At low temperature, a pair of forbidden lines due to cross terms in the spin Hamiltonian are lying between each of the main hyperfine lines (Fig. 4).<sup>49</sup> A quantitative study was performed with complex **1** at room temperature in order to determine the proportion of monomeric and dimeric species present in the solution. The spin concentration was measured using manganese(II) perchlorate in methanolic solution at various concentrations for calibration. Accordingly, only 1-1.5 % of this dimeric complex yields EPR active monomeric species in solution at room temperature.

### Grafting on silica

The above solution was used to graft the manganese complex in the nanopores of a mesoporous silica. 2D hexagonal LUS silica (MCM-41 type) prepared using cetyltrimethylammonium tosylate as surfactant was chosen as a support.<sup>50, 51</sup> It possesses a narrow

pore size distribution of  $3.8 \pm 0.1$  nm and a large mesopore volume of  $0.78 \pm 0.01$  cm<sup>3</sup> g<sup>-1</sup>. Then azide-functionalised N<sub>3</sub>-(CH<sub>2</sub>)<sub>3</sub>-Si- groups were introduced in the solid support using a molecular stencil patterning technique that allows an homogeneous distribution of the desired functions, which are separated by hydrophobic (CH<sub>3</sub>)<sub>3</sub>-Si- groups.<sup>3, 52-54</sup> The manganese complex **1** was covalently grafted by using click chemistry. As an illustrative example, the azide-functionalized silica (N<sub>3</sub>@SiO<sub>2</sub>) was reacted with **1** in a MeOH-MeCN mixture in the presence of tris-(triphenylphosphine) copper(I) bromide catalyst<sup>55</sup> to obtain the hybrid material MnL<sup>1</sup>@SiO<sub>2</sub>, with 2.5 wt % manganese. This complex loading corresponds to ~80 % yield for the click reaction. Note that the use of such a Cu(I) complex avoids the displacement of Mn(II) from L<sup>1</sup> ligand by Cu(I) during the grafting of the complex. Indeed, there are no traces of Cu(II) that would may form in aerobic conditions, according to the EPR spectrum (Fig. 4). On the other hand, the signal reveals the presence of Mn(II) as in solution. Indeed, the proportion of EPR active species remains similar to that in solution, consistent with most of the species being still dimeric. In addition, the signal is broader than in solution both at room temperature and at 116 K. Therefore, this broadening is not due to dynamic effects but to a distribution of species on the surface. This evidences the heterogeneity of the environment around the grafted species as usually observed in such hybrid materials.<sup>2</sup>

The hexagonal array of the internal pores of the material was unaltered all through the different steps of the synthesis, as shown from the X-ray diffraction patterns (Fig. 5). The decrease of pore volume from 0.78 cm<sup>3</sup> g<sup>-1</sup> down to 0.48 cm<sup>3</sup> g<sup>-1</sup> after grafting confirmed the presence of the metal complex inside the pores (ESI, Fig. S6). Concomitantly, the specific surface area underwent a diminution from 990 m<sup>2</sup> g<sup>-1</sup> to 340 m<sup>2</sup> g<sup>-1</sup>. This is consistent with partial pore filling due to internal molecular functionalization of the silica.

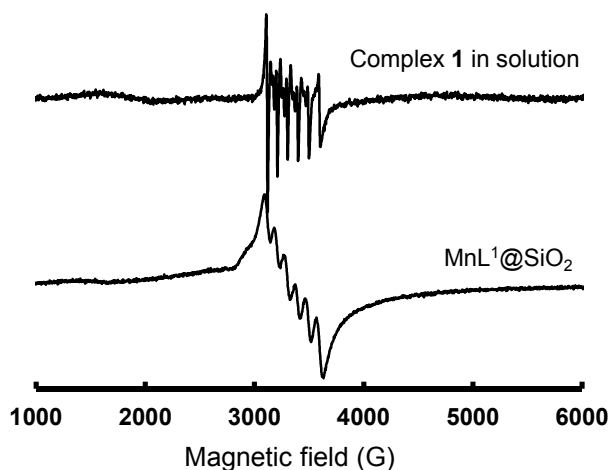


**Fig. 4** EPR spectra of **1** dissolved in a mixture MeOH/EtOH 1:1 (v/v) at 116 K and MnL<sup>1</sup>@SiO<sub>2</sub> at 298 K. Microwave frequency: 9.41 GHz, amplitude modulation: 1 G (top), 5 G (bottom), gain: 60 dB, power: 4 mW (top), 2 mW (bottom).

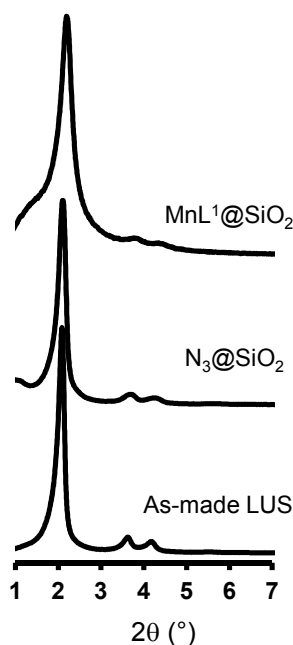


Fig. 5 X-ray diffraction patterns (powder) of LUS (mesoporous SiO<sub>2</sub> support), N<sub>3</sub>@SiO<sub>2</sub> and MnL<sup>1</sup>@SiO<sub>2</sub> materials.

## Conclusions

A series of dinuclear manganese(II) complexes with two  $\mu$ -X bridges (X = Cl, Br or N<sub>3</sub>) has been synthesised using two different clickable ligands. These ligands allow both coordination to a metal ion and also grafting on an azide-functionalized support using the Huisgen alkyne-azide cycloaddition reaction. Within this series we present the first  $\mu$ -Br bridged Mn(II) dinuclear complex for which a complete magnetic properties study has been performed. It turned out to be weakly ferromagnetic compared to the  $\mu$ -Cl analogue, which is weakly antiferromagnetic. It is also noteworthy that a better magneto-structural correlation is observed when both structural parameters ( $\theta$  and  $\Delta d$ ) are considered for the bis( $\mu_{1,1}$ -azido)dimanganese(II) complexes. Successful stabilisation of the complex mainly in its dimeric form has been achieved by grafting on mesoporous silica. This kind of hybrid nanocomposite material, where confinement is at stake, could help by comparison to better understand the catalytic mechanism of MnD. The study of the catalytic properties of these silica-supported manganese(II) complexes is under progress. Alternatively, the alkyne function present in the ligand opens other opportunities such as using these complexes as building blocks for the synthesis of metal-organic frameworks (MOFs).

## Experimental

### Synthesis of the ligands

***N,N'*-bis((pyridin-2-yl)methyl)prop-2-yn-1-amine ligand (L<sup>1</sup>).** The synthesis was based on a published protocol.<sup>28</sup> A mixture of propargylamine (1.50 g, 27.3 mmol) and potassium carbonate (22.8 g, 163.8 mmol) was stirred in 140 mL of acetonitrile for 5 min. Then 2-picolyl chloride hydrochloride (9.84 g, 60.0 mmol) dissolved in 140 mL of acetonitrile was added. The resulting

solution was stirred under reflux for 5 days. The solution was filtered and the filtrate was evaporated under reduced pressure. The resulting brown oil was dissolved in 100 mL of distilled water and extracted thrice with dichloromethane. The organic phases were gathered and dried over sodium sulphate. The solvent was finally evaporated to afford L<sup>1</sup> in 94 % yield. <sup>1</sup>H NMR (CDCl<sub>3</sub>, 300 MHz):  $\delta$  (ppm) 8.55 (ddd,  $J$  = 4.80, 1.80, 0.90 Hz, 2H), 7.64 (td,  $J$  = 7.50, 1.80 Hz, 2H), 7.50 (d,  $J$  = 7.80 Hz, 2H), 7.15 (ddd,  $J$  = 7.50, 4.80, 1.20 Hz, 2H), 3.91 (s, 4H), 3.41 (d,  $J$  = 2.40 Hz, 2H), 2.29 (t,  $J$  = 2.40 Hz, 1H). <sup>13</sup>C NMR (300 MHz, CDCl<sub>3</sub>):  $\delta$  (ppm) 158.76, 149.26, 136.47, 123.14, 122.10, 78.32, 73.62, 59.44, 42.54. IR (KBr): 3294 (w), 3062 (w), 3011 (w), 2921 (w), 2839 (w), 2095 (m, C $\equiv$ C) cm<sup>-1</sup>.

***N*-((1-methyl-1H-imidazol-2-yl)methyl)-*N*-(pyridin-2-ylmethyl)prop-2-yn-1-amine (L<sup>2</sup>).** This ligand was synthesized in two steps.

***N*-((1-Methyl-1H-imidazol-2-yl)methyl)pyrid-2-ylmethylamine:**<sup>29</sup> 2-picolylamine (2.45 g, 22.7 mmol) in 25 mL of methanol was added dropwise to a solution of 1-methyl-2-imidazolecarboxaldehyde (2.5 g, 22.7 mmol) in 50 mL of methanol. The resulting solution was stirred for 3 h at room temperature. Sodium borohydride (0.86 g, 22.7 mmol) was added portionwise and the solution was further stirred for two more hours at room temperature. The solvent was evaporated under reduced pressure and the orange oil thus obtained was redissolved in a mixture of water/methanol (25 mL/50 mL), before being extracted thrice with 50 mL of dichloromethane. The combined organic phases were washed with 50 mL of water and dried over sodium sulphate. The solvent was finally removed to obtain the product as an orange oil in 96 % yield. <sup>1</sup>H NMR (CDCl<sub>3</sub>, 300 MHz):  $\delta$  (ppm) 8.54 (ddd,  $J$  = 4.80, 1.80, 0.90 Hz, 1H), 7.63 (td,  $J$  = 7.50, 1.80 Hz, 1H), 7.31 (d,  $J$  = 7.80 Hz, 1H), 7.15 (ddd,  $J$  = 7.50, 4.80, 1.20 Hz, 1H), 6.92 (d,  $J$  = 1.20 Hz, 1H), 6.80 (d,  $J$  = 1.20 Hz, 1H), 3.93 (s, 2H), 3.89 (s, 2H), 3.66 (s, 3H).

**Synthesis of L<sup>2</sup>:** *N*-(1-methyl-1H-imidazol-2-yl)methylpyrid-2-ylmethylamine (3 g, 14.8 mmol) and potassium carbonate (8.18 g, 59.2 mmol) were dissolved in 40 mL of tetrahydrofuran. Then propargyl bromide was added dropwise, and the resulting solution was heated at 50 °C for 18 h. The solvent was removed under reduced pressure, and the brown oil thus obtained was dissolved in dichloromethane before being passed over several pads of potassium carbonate until disappearance of the hydrobromic acid. The dichloromethane was removed under reduced pressure and ligand L<sup>2</sup> was obtained in an 80 % yield. <sup>1</sup>H NMR (CDCl<sub>3</sub>, 300 MHz):  $\delta$  (ppm) 8.51 (ddd,  $J$  = 4.80, 1.80, 0.90 Hz, 1H), 7.60 (td,  $J$  = 7.50, 1.80 Hz, 1H), 7.32 (d,  $J$  = 7.80 Hz, 1H), 7.12 (ddd,  $J$  = 7.50, 4.80, 1.20 Hz, 1H), 6.88 (d,  $J$  = 1.20 Hz, 1H), 6.76 (d,  $J$  = 1.20 Hz, 1H), 3.80 (s, 2H), 3.79 (s, 2H), 3.58 (s, 3H), 3.32 (d,  $J$  = 2.40 Hz, 2H), 2.27 (t,  $J$  = 2.40 Hz, 1H). <sup>13</sup>C NMR (300 MHz, CDCl<sub>3</sub>):  $\delta$  (ppm) 158.28, 149.26, 144.59, 136.45, 127.27, 123.44, 122.21, 121.58, 78.27, 73.74, 59.29, 49.54, 42.44, 32.84. IR (KBr): 3010 (w), 2926 (w, br), 2839 (w), 2100 (m, C $\equiv$ C) cm<sup>-1</sup>.

### Synthesis of the manganese(II) complexes

**[Mn<sub>2</sub>(L<sup>1</sup>)<sub>2</sub>(Cl)<sub>2</sub>( $\mu$ -Cl)<sub>2</sub>] (1).** A solution of L<sup>1</sup> (47 mg, 0.2 mmol) in 2 mL of methanol was slowly added to a solution of MnCl<sub>2</sub> (40



mg, 0.2 mmol) in 2 mL of methanol. The solution was stirred for 1 h, and then the solid was filtered and washed with methanol to obtain 38 mg of the complex in 52 % yield. This powder was redissolved in the minimum amount of methanol, and pale yellow crystals of **1** were obtained by slow diffusion of diethylether into this solution.

**[Mn<sub>2</sub>(L<sup>1</sup>)<sub>2</sub>(Br)<sub>2</sub>(μ-Br)<sub>2</sub>] (2).** A solution of L<sup>1</sup> (47 mg, 0.2 mmol) in 2 mL of methanol was slowly added to a solution of MnBr<sub>2</sub>·4H<sub>2</sub>O (57 mg, 0.2 mmol) in 2 mL of methanol. This solution was let under stirring for 1 h. Brown crystals of **2** were obtained by slow diffusion of diethylether in the latter solution.

**[Mn<sub>2</sub>(L<sup>1</sup>)<sub>2</sub>(N<sub>3</sub>)<sub>2</sub>(μ-N<sub>3</sub>)<sub>2</sub>]·2CH<sub>3</sub>OH (3).** A solution of L<sup>1</sup> (24 mg, 0.1 mmol) in 2 mL of methanol was slowly added to a solution of Mn(NO<sub>3</sub>)<sub>2</sub>·4H<sub>2</sub>O (25 mg, 0.1 mmol) in 2 mL of methanol. The solution was stirred during 30 min, and then a solution of NaN<sub>3</sub> (26 mg, 0.4 mmol) in 3 mL of methanol was added. The mixture was further stirred for 1 h, and the solid thus formed was filtered and washed with methanol. The solid was redissolved in methanol, and slow diffusion of diethylether in that solution provided crystals suitable for X-ray diffraction.

**[Mn<sub>2</sub>(L<sup>2</sup>)<sub>2</sub>(N<sub>3</sub>)<sub>2</sub>(μ-N<sub>3</sub>)<sub>2</sub>] (4).** The synthesis is similar to the synthesis of **3**, the only difference being that L<sup>2</sup> (24 mg, 0.1 mmol) was used instead of L<sup>1</sup>. Suitable crystals for X-ray diffraction were obtained following the same diffusion protocol.

#### Synthesis of MnL<sup>1</sup>@SiO<sub>2</sub>

The manganese complex was grafted on a LUS mesoporous silica where azide functions were previously incorporated using the so-called molecular stencil patterning technique described elsewhere.<sup>53</sup>

**Mesoporous silica LUS.** A solution of cetyltrimethylammonium tosylate (CTATos) (1.96 g, 4.3 mmol) in distilled water (71 mL) was stirred at 60 °C during 1 h. In the meantime, the sodium silicate solution (49 mL) was also stirred at 60 °C during 1 h. The silicate solution was added to the surfactant one by pouring it slowly on the edge of the recipient. After a vigorous handshaking, the resulting white mixture was put in two autoclaves and heated in the microwave oven during 10 min at 180°C. The autoclaves were cooled in an ice bath during 10 min before filtration and washing with distilled water (about 100 mL). The white solid obtained was dried at 80 °C to obtain 3.1 to 3.4 g of LUS. Elemental analyses: Si (23.63%), C (30.91%), H (6.31%), N (1.72%), S (0.20%).

**N<sub>3</sub>@SiO<sub>2</sub>.** LUS silica was functionalized with trimethylsilyl functions (TMS) using a reported protocol to afford TMS@SiO<sub>2</sub>.<sup>53</sup> Then, TMS@LUS (500 mg) was pre-treated at 130°C under argon for 2 h, and at 130°C under vacuum for 2 more hours. After cooling under argon down to room temperature, a solution of 3-azidopropyl triethoxysilane (371 mg, 1.5 mmol) dissolved in 5 mL of dry toluene was added. The suspension was stirred for 1 h, 10 mL of toluene were added, and the mixture was stirred at 80 °C for 18 h. After filtration and washing with 20 mL of toluene, 20 of EtOH 70% and 20 mL of acetone, the solid was finally dried overnight at 80 °C. Elemental analysis (wt %): C: 5.18 %, H: 1.80 %, N: 2.06 %.

**MnL<sup>1</sup>@SiO<sub>2</sub>.** N<sub>3</sub>@SiO<sub>2</sub> (300 mg) was stirred in a mixture MeOH/MeCN (60 mL/20 mL). After 10 min, complex **1** (176 mg, 0.5 mmol) was added and the suspension was stirred during 1

h, before addition of CuBr(PPh<sub>3</sub>)<sub>3</sub> (93 mg, 0.10 mmol). Then the mixture was stirred at 60 °C for 6 days before filtration. The pale brown solid was washed with 200 mL of MeOH to eliminate any catalyst and unreacted species left, and dried overnight at 80 °C. Elemental analysis (wt %): C: 6.42 %, H: 1.75 %, N: 1.44 %, Mn: 2.43 %, Cl: 0.74 %.

#### Crystal structure determination and refinement

Single crystal X-ray diffraction data for **2–3** were collected at 293(2) K on a Bruker APEX II diffractometer using graphite-monochromated Mo-K<sub>α</sub> radiation while data for **1** and **4** were collected and treated on a Gemini Oxford Diffractometer at 150K and related analysis softwares.<sup>58</sup> Data reduction for **2–3** were performed with SMART and SAINT software.<sup>59</sup> The structures were solved by direct methods using SHELXS-97 program,<sup>60</sup> and refined on F<sup>2</sup><sub>s</sub> by full-matrix least-squares with SHELXL-97 program included in the WINGX software package.<sup>60, 61</sup> Absorption correction was applied using SADABS.<sup>62</sup> For complexes **1** and **4**, an absorption correction based on the crystal faces was applied to the data sets (analytical).<sup>63</sup> Structures of **1** and **4** were solved by direct methods combined with Fourier difference syntheses and refined against *F* using reflections with [*I*/*σ*(*I*)>3] by using the CRYSTALS program.<sup>64</sup> All non-hydrogen atoms were refined using anisotropic terms. The hydrogen atoms were placed at calculated positions and refined with isotropic parameters as riding atoms. The hydrogen atoms for the co-crystallized methanol molecules were located from difference maps for complex **3**. The final geometrical calculations and the graphical manipulations were carried out with PARST95,<sup>65</sup> PLATON,<sup>66</sup> (for complexes **2–4**) and DIAMOND<sup>67</sup> programs.

Crystal data, refinement results, atomic coordinates, selected bond lengths and bond angles for **1–4** are summarized in Tables S1-S12.

#### Physical characterization

Infrared spectra were recorded from KBr pellets using a Mattson 3000 IRTF spectrometer. Nitrogen sorption isotherms at 77 K were determined with a volume device Belsorp Max on solids that were dried at 80 °C under vacuum overnight. Low angle X-ray powder diffraction (XRD) experiments were carried out using a Bruker (Siemens) D5005 diffractometer using Cu K monochromatic radiation. Variable-temperature magnetic susceptibility measurements were made using a Quantum Design SQUID susceptometer, using an applied field of 1000 G. Diamagnetic corrections of the constituent atoms were estimated from Pascal constants. EPR spectra were recorded using a Bruker Eleksys e500 X-band (9.4 GHz) spectrometer with a standard cavity. The EPR calibration was performed using manganese(II) perchlorate as spin reference in the same range of concentrations as in the samples. The spin quantification was performed by double integration of the signal. The simulated spectra were calculated using EasySpin toolbox from Matlab.

#### Acknowledgements

L. Khrouz is greatly acknowledged for recording and analysing the EPR spectra. J. C. thanks the French “Ministère de l’enseignement, de la recherche et de la technologie” (MERT) for

a PhD fellowship, and the C-MIRA program of Rhône-Alpes region in France for financial support to the collaboration between the Universitat de València (Spain) and the Ecole Normale Supérieure de Lyon (France). The Spanish work was supported by the MICINN (Spain) (Project CTQ2010-15364) and the Generalitat Valenciana (Spain) (Projects PROMETEO/2009/108, and ISIC/2012/002). A part of this work was supported by the Fundo Europeu de Desenvolvimento Regional-QREN-Compete (Project PTDC/FIS/102284/2008) and the Fundação para a Ciência e Tecnologia (Project PEst-C/FIS/UI0036/2011).

## Notes and references

<sup>a</sup> Instituto de Ciencia Molecular, Universitat de València, C/ Catedrático José Beltrán 2, 46980 Paterna, València, Spain. Fax: +34-963 543 274; Tel: +34-963 544 439; E-mail: isabel.castro@uv.es

<sup>b</sup> Laboratoire de Chimie, Ecole Normale Supérieure de Lyon, University of Lyon, 46 Allée d'Italie, 69364 Lyon cedex 07, France. Fax: +33-472 72 88 60; Tel: +33-472 72 88 56; E-mail: belen.albela@ens-lyon.fr

<sup>c</sup> Physics Department, Universidade de Coimbra, Rua Larga, P-3004-516 Coimbra, Portugal.

<sup>d</sup> Laboratoire des Multimatériaux et Interfaces, UMR 5615 CNRS-Université Claude Bernard Lyon 1, 43 boulevard du 11 novembre 1918, 69622 Villeurbanne cedex, France.

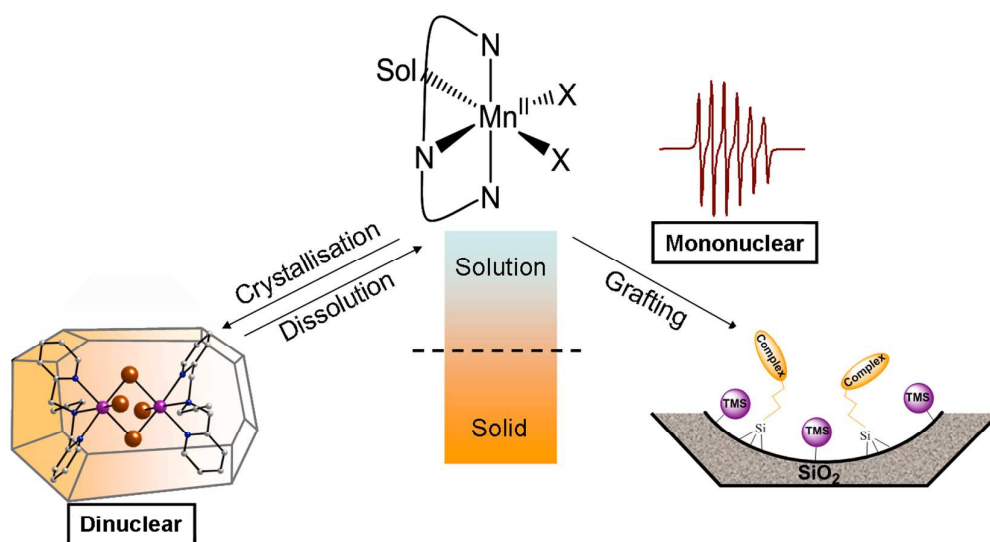
† Electronic Supplementary Information (ESI) available: crystallographic details of the complexes, crystal packing figures of 1-4, EPR simulation of I and N<sub>2</sub> sorption isotherms of the porous materials. CCDC 905065, CCDC 911104, CCDC 911105 and CCDC 911106 contain the supplementary crystallographic data for 1-4, respectively. For ESI and crystallographic data in CIF or other electronic format see DOI: 10.1039/b000000x/

- T. J. Terry and T. D. P. Stack, *J. Am. Chem. Soc.*, 2008, 130, 4945-4953.
- S. Abry, A. Thibon, B. Albela, P. Delichère, F. Banse and L. Bonneviot, *New J. Chem.*, 2009, 33, 484-496.
- S. Calmettes, B. Albela, O. Hamelin, S. Menage, F. Miomandre and L. Bonneviot, *New J. Chem.*, 2008, 32, 727-737.
- H. C. Kolb, M. G. Finn and K. B. Sharpless, *Angew. Chem. Int. Ed.*, 2001, 40, 2004-2021.
- H. C. Kolb and K. B. Sharpless, *Drug Discov. Today*, 2003, 8, 1128-1137.
- J. E. Moses and A. D. Moorhouse, *Chem. Soc. Rev.*, 2007, 36, 1249-1262.
- L. Nebhani and C. Barner-Kowollik, *Adv. Mater.*, 2009, 21, 3442-3468.
- F. Santoyo-Gonzalez and F. Hernandez-Mateo, *Chem. Soc. Rev.*, 2009, 38, 3449-3462.
- C. Chu and R. Liu, *Chem. Soc. Rev.*, 2011, 40, 2177-2188.
- B. S. Rana, S. L. Jain, B. Singh, A. Bhaumik, B. Sain and A. K. Sinha, *Dalton Trans.*, 2010, 39, 7760-7767.
- S. L. Jain, B. S. Rana, B. Singh, A. K. Sinha, A. Bhaumik, M. Nandi and B. Sain, *Green Chem.*, 2010, 12, 374-377.
- E. A. Lewis and W. B. Tolman, *Chem. Rev.*, 2004, 104, 1047-1076.
- L. M. Mirica, X. Ottenwaelder and T. D. P. Stack, *Chem. Rev.*, 2004, 104, 1013-1045.
- E. I. Solomon, U. M. Sundaram and T. E. Machonkin, *Chem. Rev.*, 1996, 96, 2563-2605.
- P. C. A. Bruijninx, G. van Koten and R. J. M. K. Gebbink, *Chem. Soc. Rev.*, 2008, 37, 2716-2744.
- J. P. Emerson, M. L. Wagner, M. F. Reynolds, L. Que, M. J. Sadowsky and L. P. Wackett, *J. Biol. Inorg. Chem.*, 2005, 10, 751-760.
- T. D. H. Bugg and S. Ramaswamy, *Curr. Opin. Chem. Biol.*, 2008, 12, 134-140.
- L. Que and M. F. Reynolds, *Met. Ions Biol. Syst.*, 2000, 37, 505-525.
- F. H. Vaillancourt, J. T. Bolin and L. D. Eltis, *Crit. Rev. Biochem. Mol. Biol.*, 2006, 41, 241-267.
- A. K. Whiting, Y. R. Boldt, M. P. Hendrich, L. P. Wackett and L. Que, *Biochemistry*, 1996, 35, 160-170.
- M. W. Vetting, L. P. Wackett, L. Que, J. D. Lipscomb and D. H. Ohlendorf, *J. Bacteriol.*, 2004, 186, 1945-1958.
- V. Georgiev, T. Borowski and P. E. M. Siegbahn, *J. Biol. Inorg. Chem.*, 2006, 11, 571-585.
- J. P. Emerson, E. G. Kovaleva, E. R. Farquhar, J. D. Lipscomb and L. Que, *PNAS*, 2008, 105, 7347-7352.
- K. D. Koehntop, J. P. Emerson and L. Que, *J. Biol. Inorg. Chem.*, 2005, 10, 87-93.
- M. J. Carney, N. J. Robertson, J. A. Halfen, L. N. Zakharov and A. L. Rheingold, *Organometallics*, 2004, 23, 6184-6190.
- D. E. Bergbreiter, P. N. Hamilton and N. M. Koshti, *J. Am. Chem. Soc.*, 2007, 129, 10666-10667.
- S. Huang, R. J. Clark and L. Zhu, *Org. Lett.*, 2007, 9, 4999-5002.
- J. Rosenthal and S. J. Lippard, *J. Am. Chem. Soc.*, 2010, 132, 5536-5537.
- T. Dhanalakshmi, E. Suresh and M. Palaniandavar, *Dalton Trans.*, 2009, 38, 8317-8328.
- I. Romero, M. N. Collomb, A. Deronzier, A. Llobet, E. Perret, J. Pecaut, L. Le Pape and J. M. Latour, *Eur. J. Inorg. Chem.*, 2001, 69-72.
- J. Z. Wu, E. Bouwman, A. M. Mills, A. L. Spek and J. Reedijk, *Inorg. Chim. Acta*, 2004, 357, 2694-2702.
- G. A. van Albada, A. Mohamadou, W. L. Driessen, R. de Gelder, S. Tanase and J. Reedijk, *Polyhedron*, 2004, 23, 2387-2391.
- O. Seewald, U. Florke, G. Henkel and T. Seshadri, *Acta Crystallogr. Section E: Struct. Rep. Online*, 2005, 61, m1948-m1950.
- C. M. Liu, S. Gao, D. Q. Zhang, Z. L. Liu and D. B. Zhu, *Inorg. Chim. Acta*, 2005, 358, 834-838.
- J. Qian, W. Gu, S. P. Yan, D. Z. Liao and P. Cheng, *Acta Crystallogr. Section E: Struct. Rep. Online*, 2007, 63, m687-m688.
- M. M. Yu, Z. H. Ni, C. C. Zhao, A. L. Cui and H. Z. Kou, *Eur. J. Inorg. Chem.*, 2007, 5670-5676.
- H. Y. Wu, H. Q. An, B. L. Zhu, S. R. Wang, S. M. Zhang, S. H. Wu and W. P. Huang, *Inorg. Chem. Commun.*, 2007, 10, 1132-1135.
- O. Kahn, *Molecular Magnetism*, Wiley-VCH, 1993.
- J. Cano, University of Valencia, Valencia, Spain, 2003.
- (a) R. Herchel, R. Boca, M. Gembicky, K. Falk, H. Fuess, W. Haase and I. Svoboda, *Inorg. Chem.*, 2007, 46, 1544. (b) R. Boca, *Coord. Chem. Rev.*, 2004, 248, 757.
- E. Ruiz, J. Cano, S. Alvarez and P. Alemany, *J. Am. Chem. Soc.*, 1998, 120, 11122-11129.

42. V. H. Crawford, H. W. Richardson, J. R. Wasson, D. J. Hodgson and W. E. Hatfield, *Inorg. Chem.*, 1976, 15, 2107-2110.
43. T. K. Karmakar, B. K. Ghosh, A. Usman, H. K. Fun, E. Riviere, T. Mallah, G. Aromi and S. K. Chandra, *Inorg. Chem.*, 2005, 44, 2391-2399.
44. R. Cortes, J. L. Pizarro, L. Lezama, M. I. Arriortua and T. Rojo, *Inorg. Chem.*, 1994, 33, 2697-2700.
45. Z. H. Ni, H. Z. Kou, L. Zheng, Y. H. Zhao, L. F. Zhang, R. J. Wang, A. L. Cui and O. Sato, *Inorg. Chem.*, 2005, 44, 4728-4736.
46. A. Das, G. M. Rosair, M. S. El Fallah, J. Ribas and S. Mitra, *Inorg. Chem.*, 2006, 45, 3301-3306.
47. J. L. Manson, A. M. Arif and J. S. Miller, *Chem. Commun.*, 1999, 1479-1480.
48. M. A. M. Abu-Youssef, A. Escuer, D. Gatteschi, M. A. S. Goher, F. A. Mautner and R. Vicente, *Inorg. Chem.*, 1999, 38, 5716-5723.
49. B. Bleaney and R. S. Rubins, *Proc. Phys. Soc.*, 1961, 77, 103-112.
50. J. S. Beck, J. C. Vartuli, W. J. Roth, M. E. Leonowicz, C. T. Kresge, K. D. Schmitt, C. T. W. Chu, D. H. Olson, E. W. Sheppard, S. B. McCullen, J. B. Higgins and J. L. Schlenker, *J. Am. Chem. Soc.*, 1992, 114, 10834-10843.
51. P. Reinert, B. Garcia, C. Morin, A. Badiei, P. Perriat, O. Tillement and L. Bonneviot, in *Nanotechnology in Mesosstructured Materials*, Elsevier Science Bv, Amsterdam, 2003, vol. 146, pp. 133-136.
52. S. Abry, B. Albela and L. Bonneviot, *C. R. Chim.*, 2005, 8, 741-752.
53. A. Badiei, L. Bonneviot, N. Crowther and G. M. Ziarani, *Journal Organomet. Chem.*, 2006, 691, 5911-5919.
54. K. Zhang, B. Albela, M. Y. He, Y. M. Wang and L. Bonneviot, *Phys. Chem. Chem. Phys.*, 2009, 11, 2912-2921.
55. K. Bueglova, N. Moitra, J. Hodacova, X. Cattoen and M. W. C. Man, *J. Org. Chem.*, 2011, 76, 7326-7333.
56. V. Georgiev, T. Borowski, M. R. A. Blomberg and P. E. M. Siegbahn, *J. Biol. Inorg. Chem.*, 2008, 13, 929-940.
57. M. Savonnet, E. Kockrick, A. Camarata, D. Bazer-Bachi, N. Bats, V. Lecocq, C. Pinel and D. Farrusseng, *New J. Chem.*, 2011, 35, 1892-1897.
58. CrysAlisPro, v. 1.171.33.46, Oxford Diffraction Ltd., 2009.
59. Bruker, SMART and SAINT, Bruker AXS Inc., Madison, Wisconsin, USA, 2003.
60. G. M. Sheldrick, SHEXL-97 and SHELXS-97, University of Göttingen, Germany, 1998.
61. L. J. Farrugia, *J. Appl. Crystallogr.*, 2012, 45, 849-854.
62. G. M. Sheldrick, SADBAS, University of Göttingen, Germany, 2003.
63. J. Der Meulen and H. Tompa, *Acta Crystallogr.*, 1965, 19, 1014-1018.
64. D. J. Watkin, C. K. Prout, J. R. Carruthers, P. W. Betteridge and R. I. Cooper, CRYSTALS Issue 11, Chemical Crystallography Laboratory, University of Oxford, Oxford, UK, 1999.
65. M. Nardelli, *J. Appl. Crystallogr.*, 1995, 28, 659-659.
66. A. L. Spek, *Acta Crystallogr. Sect. A*, 1990, 46, c34.
67. K. Brandenburg and H. Putz, DIAMOND 2.1d, Crystal Impact GbR, Bonn, Germany, 2000.

## Bioinspired manganese(II) complexes with a clickable ligand for immobilization on a solid support

Jérémy Chaignon, Salah-Eddine Stiriba, Francisco Lloret, Consuelo Yuste, Guillaume Pilet, Laurent Bonneviot, Belén Albela,\* and Isabel Castro\*



A new series of dinuclear manganese(II) complexes with two bioinspired ligands that mimic the active site of the MndD have been prepared. These ligands possess an alkyne side function that allows for an efficient grafting in a solid support using click chemistry. The complexes are characterised by a weak magnetic exchange interaction between the two high-spin Mn<sup>II</sup> ions through the two X<sup>-</sup> bridges ( $J$  in the range of  $-0.059$  to  $+5.30$  cm<sup>-1</sup>). Successful stabilisation of complexes mainly in its dimeric form has been achieved by grafting on mesoporous silica of MCM-41 type.